An epoxide hydrolase involved in the biosynthesis of an insect sex attractant and its use to localize the production site

Mohatmed Abdel-latief*, Leif A. Garbe†, Markus Koch*, and Joachim Ruther*‡

*Institut für Biologie, Freie Universität Berlin, Haderslebener Str. 9, D-12163 Berlin, Germany; and †Institut für Biotechnologie, Technische Universität Berlin, Seestraβe 13, D-13353 Berlin, Germany

Edited by Wendell Roelofs, Cornell University, Geneva, NY, and approved April 17, 2008 (received for review February 16, 2008)

Epoxide hydrolases (EHs) are enzymes occurring in virtually any living organism. They catalyze the hydrolysis of epoxide containing lipids and are involved in crucial mechanisms, such as the detoxification of xenobiotics or the regulation of inflammation and blood pressure. Here, we describe a function of a putative EH gene in the biosynthesis of a sex attractant in the jewel wasp *Nasonia vitripennis* and use this gene to localize the site of pheromone production. Males of this parasitic wasp release a mixture of (4*R*,5*R*)-(═threo-) and (4*R*,5*S*)-(═erythro-)5-hydroxy-4-decanolide (HDL) to attract virgin females. Using a stable isotope labeled precursor, we demonstrated that vernolic acid (═*erythro*-12,13-epoxy-octadec-9*Z*-enoic acid) is converted by *N. vitripennis* males to threo-HDL. This suggested the involvement of an EH in hydrolyzing the fatty acid epoxide under inversion of the stereochemistry into the respective diol, which might be further processed by chain shortening and lactonization to HDL. We cloned a putative *N. vitripennis* EH gene (*Nasvi-EH1*) encoding 470 amino acids and localized its transcripts in the male rectal papillae by *in situ* RT-PCR. Chemical analyses and histological studies confirmed that males synthesize the sex attractant in the rectal vesicle and release it via the anal orifice. Involvement of *Nasvi-EH1* in HDL biosynthesis was established by RNAi-mediated gene silencing. Injection of *Nasvi-EH1* dsRNA into male abdomens inhibited pheromone biosynthesis by 55% and suppressed the targeted gene transcripts in the rectal vesicle by 95%.

Nasonia vitripennis | pheromone biosynthesis | pheromone gland

Chemical communication by pheromones is probably the most important method by which insects communicate with conspecifics (1, 2). Insects contain a plethora of exocrine glands where chemical messengers are produced (3). Our current understanding of the biosynthesis of insect pheromones is largely based on studies investigating moths, flies, cockroaches, and beetles (4, 5). Early studies on insect pheromone biosynthesis focused on the identification of precursors and intermediates by using isotope labeling techniques (6, 7). Other approaches studied the endocrine regulation of pheromone biosynthesis (8, 12) and aimed at the characterization of biosynthetic enzymes (4, 5, 13). The tremendous progress of molecular methods during the past years and the availability of genome sequences of various model organisms shifted the interests of researchers more and more toward the genes involved in pheromone biosynthesis (14–20). Particularly, the use of RNA interference (RNAi)-mediated gene silencing and *in situ* RT-PCR has demonstrated the usefulness of these cutting edge tools for insect pheromone research, because they allow both the unequivocal assignment of gene function *in vivo* and cell localization of biosynthetic pathways within the organism (21–23).

Many insects have modified pathways of the primary metabolism to produce pheromones and particularly the fatty acid metabolism is of central importance. For instance, most of the well studied sex attractants of moths are synthesized from saturated fatty acids by the interplay of desaturases, elongases, and other enzymes catalyzing chain shortening, epoxidation, or the introduction and modification of other functional groups (5, 13, 24).

Epoxide hydrolases (EHs) are widespread in nature and catalyze the hydrolysis of epoxides to vicinal diols. Most of these enzymes have important functions for the respective organisms being involved in the detoxification of xenobiotics, inflammation, and blood pressure regulation in mammals or the cutin biosynthesis in plants (25, 26). In insects, EHs have been shown to degrade juvenile hormones (27, 28) and to deactivate epoxide containing sex pheromones in moth antennae (29). In the context of pheromone biosynthesis, however, these enzymes have not, to our knowledge, been studied.

Compared with other insect taxa, little is known about the biosynthetic pathways of hymenopteran pheromones (30–33), and, apparently, no efforts have been undertaken so far to decipher pheromone biosynthesis in parasitic wasps, despite the importance of this species-rich group of carnivorous insects as natural enemies (34). A model organism for the study of parasitic wasp biology is the jewel wasp *Nasonia vitripennis* (Hymenoptera: Pteromalidae) (35). Females of this parasitic wasp lay their eggs into the puparia of cyclorraphous fly species, where hatching larvae develop gregariously feeding on the host pupa (36). Males of *N. vitripennis* release a mixture of (4*R*,5*R*)-(═threo-) and (4*R*,5*S*)-(═erythro-)5-hydroxy-4-decanolide (HDL) to attract females (37). This response is shown by virgin females only and is synergized by the trace component 4-methylquinazoline (4-MeQ) (38). Both HDL and 4-MeQ occur in the abdomen of males, but the exact site of pheromone production is still unknown. (4*R*,5*R*)-HDL was found as a major metabolite in cultures of the yeast *Sporobolomyces odorus* after addition of vernolic acid (VA) [═(−)-*erythro*-12,13-epoxy-octadec-9*Z*-enoic acid], suggesting the involvement of an EH hydrolyzing the fatty acid epoxide to the respective diol, which after chain shortening and lactonization may lead to (4*R*,5*R*)-HDL (39). In the present integrative study, we localize the pheromone producing gland in the abdomen *N. vitripennis* males and investigate whether they can use VA as a pheromone precursor. We also report the molecular characterization of a putative EH gene involved in pheromone biosynthesis and identify the pheromone producing tissue by cell localization of the EH gene transcripts.

Author contributions: M.A.-l. and J.R. designed research; M.A.-l., L.A.G., M.K., and J.R. performed research; L.A.G. contributed new reagents/analytic tools; M.A.-l. and J.R. analyzed data; and M.A.-l. and J.R. wrote the paper.

The authors declare no conflict of interest.

This article is a PNAS Direct Submission.

Data deposition: The sequence reported in this paper has been deposited in the GenBank database [accession no. EU441215 (*Nasonia vitripennis Nasvi-EH1*].

‡To whom correspondence should be addressed. E-mail: ruther@zedat.fu-berlin.de.

This article contains supporting information online at www.pnas.org/cgi/content/full/0801559105/DCSupplemental.

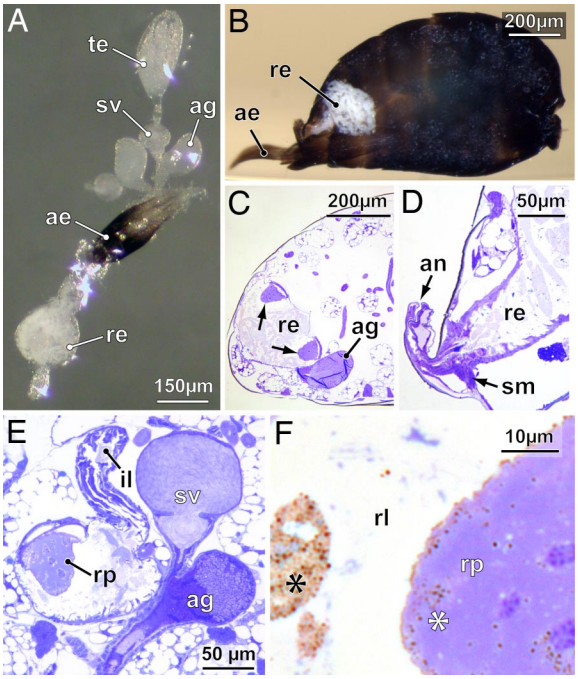

Fig. 1. Male reproductive system and hindgut of *N. vitripennis*. (*A*) Whole-mount of the dissected components used for localizing the pheromone gland. (*B*) View into a sagittally sliced abdomen in resin, showing the rectum filled with a whitish tubular accumulation (meconium). (*C* and *D*) Sagittal sections of the abdomen at two different levels, showing two rectal papillae (arrows) protruding into the rectal vesicle (*C*) and the opening of the rectum to the exterior via the anus, which can be dilated by rectal suspensory muscles (*D*). (*E*) Transverse section through rectal vesicle and right gonad, showing the rectal papilla flexibly attached to a strengthened muscular cap. (*F*) Detail of rectal papilla, showing vesicles (asterisks) both within the cone cells of the rectal papilla and aggregated in the lumen of the rectal vesicle. ae, aedeagus; ag, accessory gland; an, anus; il, ileum; re, rectum; rl, rectal lumen; rp, rectal papilla; sm, suspensory muscle (dilator); sv, seminal vesicle; te, testis.

Results

To localize the site of pheromone production in the male abdomen, we excised the abdominal tip of males and extracted the adjacent rectal vesicle and interior genitalia (testis, seminal vesicle, and accessory gland) separately (Fig. 1*A*). Both HDL diastereomers (threo: 80 ± 27 ng/gland, erythro: 160 ± 55 ng/gland) and 4-MeQ (6.0 ± 0.6 ng/gland) were found in the rectal vesicle but were absent from genitalia extracts (Fig. 2). To study the role of VA as a putative pheromone precursor, we synthesized fully ^{13}C-labeled racemic (±)-erythro-VA and applied it as acetone solution to the abdomial tip of *N. vitripennis* males. The pheromone was extracted 18 h later and analyzed by GC-MS. Mass spectra revealed incorporation of ^{13}C into threo-HDL (25 ± 5%) as indicated by mass shifts of four diagnostic ions (Fig. 3). The mass peak (*m/z* 186) shifted to *m/z* 196 because of the complete incorporation of ^{13}C into the molecule. α-Cleavage between the lactone ring and the side chain leads to the two diagnostic ions *m/z* 86 (base peak, note the rearrangement of a proton) and *m/z* 101, which shifted upon labeling to *m/z* 90 and *m/z* 107, respectively. Finally, the ion *m/z* 115 resulting from α-cleavage between C_5 and C_6 shifted to *m/z* 120. No ^{13}C-incorporation was measurable in erythro-HDL. Application of the pure solvent had no detectable influence on the mass spectra of both HDL-diastereomers. These data demonstrate that *N. vitripennis* males are able to convert (±)-erythro-VA to threo-HDL and suggest the involvement of an EH catalyzing the hydrolysis of

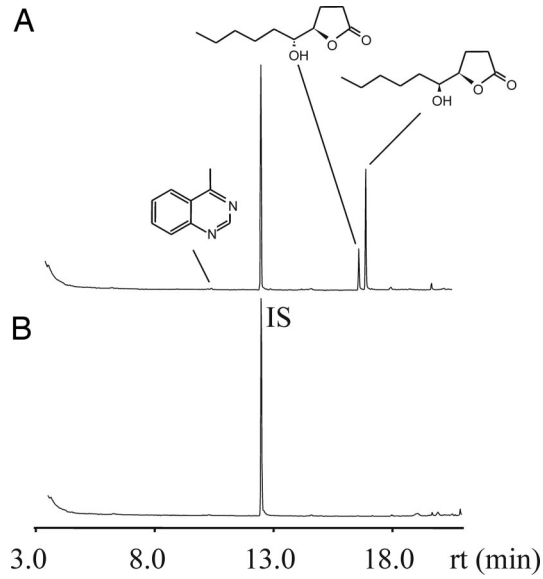

Fig. 2. Localization of the pheromone gland in the male abdomen. Total ion current chromatograms of dichloromethane extracts from rectal vesicle (*A*) and interior genitalia (testis, seminal vesicle, and accessory gland) (*B*) of a single *N. vitripennis* male. IS indicates the internal standard (20 ng of methyl undecanoate).

the fatty acid epoxide to the respective diol with inversion of stereochemistry at the site of epoxide opening.

We cloned a putative EH from *N. vitripennis*, using degenerated primers (Nas.EH1.dF1-Nas.EH1.dR1) corresponding to the abhydrolase_1 domain of *Apime-EH* from *Apis mellifera* [supporting information (SI) Fig. S1]. Initially, a DNA fragment of 356 bp was obtained matching in its sequence a clone from the *Nasonia* genome (GenBank accession no. XP_001602953). From these data, we designed the specific primers Nas.EH1.F/R1, 2, 3, and 4 (Fig. S1) that were used in different PCRs to amplify the complete gene DNA. The *Nasvi-EH1* gene was assembled by overlapping the amplified DNA fragments. The full-length cDNA of *Nasvi-EH1* is 1,413 bp and encodes 470 amino acids with a calculated molecular mass of 53.71 kDa (Fig. S1).

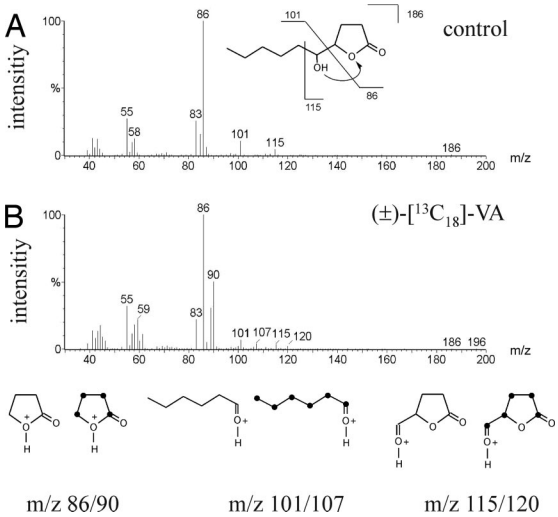

Fig. 3. Mass spectral data for threo-HDL from *N. vitripennis* obtained after application of 0.1 µl of acetone (control) (*A*) and (±)-[$^{13}C_{18}$]-vernolic acid (*B*). Pairs of diagnostic ions indicating the incorporation of the labeled precursor are shown below. ^{13}C-Atoms are represented by black dots.

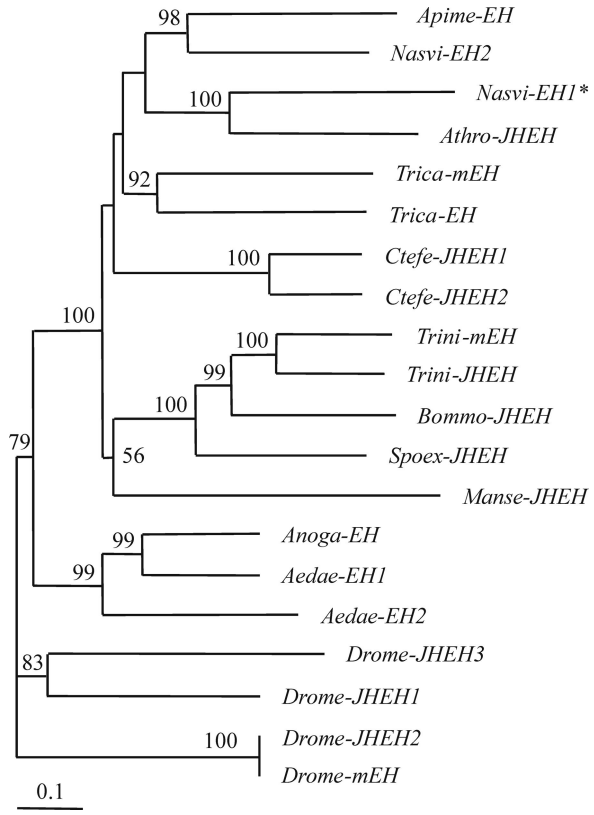

Fig. 4. Phylogenetic tree analysis of insect epoxide hydrolase genes. The asterisk indicates the putative EH from *N. vitripennis* (*Nasvi-EH1*). N, *vitripennis* (*Nasvi-EH2*), *Apis mellifera* (*Apime-EH*), *A. rosae* (*Athro-JHEH*), *Manduca sexta* (*Manse-JHEH*), *Bombyx mori* (*Bommo-JHEH*), *Spodoptera exigua* (*Spoex-JHEH*), *Trichoplusia ni* (*Trini-mEH*, and *EH*), *Drosophila melanogaster* (*Drome-JHEH1*, *2*, and *3* and *mEH*), *Aedes aegypti* (*Aedae-JHEH1*, and *2*), *Ctenocephalides felis* (*Canfe-EH1*, and *2*), and *Tribolium castaneum* (*Trica-EH*, and *mEH*). The amino acid alignment (shown in Fig. S5) was carried out by using CLUSTAL W. The corrected distance tree was rooted by declaring the *D. melanogaster* (*Drome-mEH*) and its homolog (*Drome-JHEH*) as outgroup based on its role as homolog to insect JHEH (26). The neighbor-joining tree was produced by using the PHYLIP package and based on the consensus of 1,000 bootstrap replicates. Numbers above branches are the whole percentage values of 1,000 neighbor-joining bootstraps. Tree drawing was performed with the help of TreeView 1.6.6.

Exon/intron analysis showed that the *Nasvi-EH1* gene has five introns that are potential alternative splicing sites that may yield different mRNA isoforms (Table S1). Analysis of the deduced amino acid sequence revealed that *Nasvi-EH1* is a typical EH protein with a characteristic EH domain architecture. In general, *Nasvi-EH1* showed a homology of >40% to other insect EHs at the amino acid level and shared the highest identity with *Apime-EH* (59%) (Fig. S2) followed by the juvenile hormone degrading *Athro-JHEH* from *Athalia rosae* (51%). The same was true for the N terminus (EHN) (71% for *Apime-EH*, 48% for *Athro-JHEH*) and abhydrolase_1 (64% *Apime-EH* for and 58% *Athro-JHEH*) domains. Phylogenetic tree analysis showed that hymenopteran EHs are structurally closely related and represent orthologs to EH genes from other insect taxa (Fig. 4).

Functional involvement of *Nasvi-EH1* in HDL biosynthesis was established by RNA interference (RNAi) experiments. We synthesized dsRNA corresponding to the *Nasvi-EH1* gene and injected it into freshly emerged *N. vitripennis* males. The pheromone titer was determined 48 h later and compared with control males injected either with dsRNA corresponding to *Nasvi-EH2*, a second EH gene from *N. vitripennis* (gene bank

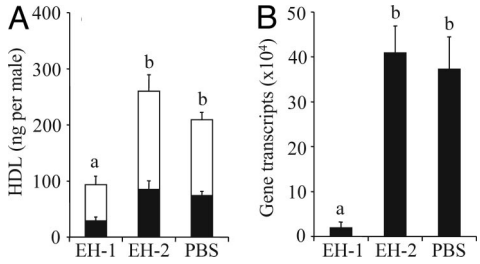

Fig. 5. Effects of RNAi treatment on HDL titers of *N. vitripennis* males (threo-HDL, black proportion of columns; erythro-HDL, white proportion of columns) (*A*) and the quantity of targeted *Nasvi-EH1* gene transcripts in male rectal vesicles (*B*) as estimated by quantitative real time RT-PCR analysis. For RNAi treatment, males were injected with dsRNA corresponding to *Nasvi-EH1* (EH1), and control males were injected with dsRNA corresponding to *Nasvi-EH2* (EH2) or 1× DEPC-PBS buffer (PBS). Lowercase letters indicate significant differences between treatments (one-way ANOVA, least significant difference test).

accession no. XP_001602953) or with 1× DEPC-PBS buffer only. Males injected with *Nasvi-EH1* dsRNA had significantly lower titers of both threo- and erythro-HDL than the controls (threo: $F_{2,66} = 7.189$, $P = 0.0015$; erythro: $F_{2,66} = 7.246$, $P = 0.0014$, one-way ANOVA) (Fig. 5*A*). The impact of RNAi treatment was also studied on the transcriptional level by quantitative real time RT-PCR, using RNA samples from individual rectal vesicles as template. Injection of *Nasvi-EH1* dsRNA decreased the targeted *Nasvi-EH1* gene transcripts in the male rectal vesicle by ≈95% when compared with the control males injected with *Nasvi-EH2* dsRNA or DEPC-PBS buffer ($F_{2,15} = 94{,}938$, $P < 0.001$, one-way ANOVA) (Fig. 5*B*). In another control experiment, injection of *Nasvi-EH1* dsRNA did not influence gene transcripts of the nontarget gene *Nasvi-EH2* ($t = 0.440$, df = 5, $P = 0.678$, t test for independent samples, Fig. S3).

To identify the pheromone producing cells within the rectal vesicle, we performed whole-mount *in situ* RT-PCR analyses. *Nasvi-EH1* mRNA was localized in the rectal papillae of 2-day old males but was absent in females of the same age (Fig. 6 *A* and *B*). No signal was found in the technical control experiment (data not shown).

Histological studies of the male rectal papillae revealed structural differences to data for females published in ref. 40. These

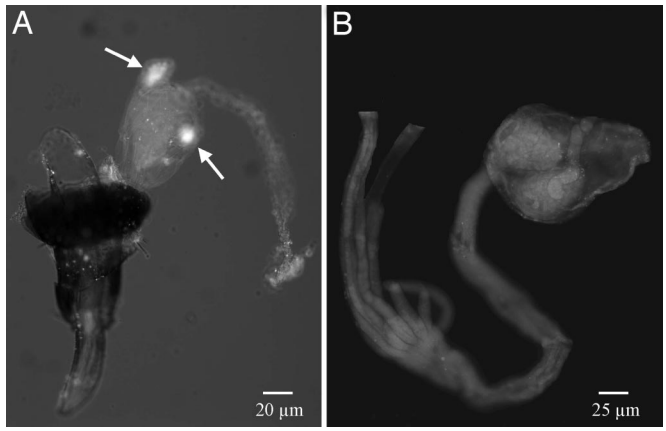

Fig. 6. Tissue-specific localization of the *N. vitripennis* epoxide hydrolase gene (*Nasvi-EH1*), using whole-mount *in situ* RT-PCR analysis. (*A*) *Nasvi-EH1* was localized in the male rectal papillae. (*B*) No expression signal was detected in females. Sites of localization are signed with arrows. The *Nasvi-EH1* mRNAs were labeled by using Dig 11-dUTP and visualized by fluorescence *in situ* RT-PCR analysis, using HNPP/Fast Red TR.

differences concern the apparent absence of a central cavity within the cone-shaped papillae and the presence of a thickened muscular cap to which the papillae are flexibly attached (Fig. 1 *C* and *E*). Distally, the cone cells of the male rectal papillae accumulate small vesicles beneath the apical cell membrane (Fig. 1*F*), which we suggest are pheromone droplets. Strikingly, these droplets were found in several aggregations within the lumen of the male rectum around a tubular mass of excrements (meconium) (Fig. 1*B*). Unlike in some Braconidae (41), the rectum of *N. vitripennis* males is not fused with any abdominal tergite but conventionally tapers off into the anus, which therefore may be used for pheromone release (Fig. 1*D*).

Discussion

The results of our labeling experiment clearly demonstrate that *N. vitripennis* males are able to convert (±)-erythro-VA into threo-HDL and strongly suggest that it is the precursor of this pheromone component in nature. In plants, erythro-VA has been shown to derive from stereospecific epoxidation of linoleic acid by cytochrome P450 enzymes (42) and is a typical substrate for EHs that hydrolyze the erythro-epoxide to the respective threo-diol. Hence, hydrolysis is typically accompanied by inversion of stereochemistry at the site of epoxide opening (43). In yeast cells, threo-HDL has been obtained as a major product after addition of either erythro-VA or the respective threo-dihydroxylated fatty acids (39, 44). We assumed a similar biosynthetic pathway also in *N. vitripennis* and, therefore, performed a targeted search for EH genes resulting in the identification of *Nasvi-EH1*, which was shown to be highly homologous to other insect EHs. We conclude that *Nasvi-EH1* is functionally involved in the pheromone biosynthesis of *N. vitripennis* males because we were able to disrupt the gene by RNAi as indicated by clearly reduced pheromone titers and *Nasvi-EH1* gene transcripts in the pheromone producing tissue. Male pheromone titers after injection of *Nasvi-EH1* dsRNA were still relatively high (≈50% of the normal level), suggesting that precursor compounds can be "plugged in" the pathway downstream of *Nasvi-EH1* or another enzyme can take over the function of *Nasvi-EH1*. However, our data suggest that this is not case for *Nasvi-EH2* because RNAi, using this gene, had no effect on male pheromone titers.

We determined the site of biosynthesis to be the rectal vesicle because this gland contained both HDL and the minor pheromone component 4-MQ (37, 38). The line of arguments of our integrative study was closed by the gender-specific cell localization of *Nasvi-EH1* gene transcripts in male rectal papillae, which, like the final product HDL, were disrupted by injection of dsRNA into the male abdomen.

Our experiments suggested that *Nasvi-EH1* is involved in the biosynthesis of both HDL diastereomers, because threo- and erythro-HDL titers were influenced by RNAi. However, the labeling experiment revealed that erythro-VA does not function as a precursor for erythro-HDL. Therefore, we conclude that the two HDL diastereomers cannot be converted into each other, e.g., by an oxidoreductase; instead, erythro-HDL is derived from another epoxide precursor. We suggest this to be a threo-configurated fatty acid epoxide that can be derived from epoxidation of trans- unsaturated fatty acids and is hydrolyzed under inversion at the site of water attack to the respective erythro-diol (45, 46).

The role of *Nasvi-EH1* in the biosynthesis of an insect sex attractant adds another facet to the multitude of essential functions this family of enzymes has in nature (25, 26). EHs introduce vicinal hydroxyl groups into fatty acid chains, one of which is necessary for lactonization in *N. vitripennis*. Fatty acid derived γ-lactones have also been found as sex pheromones in some scarab beetles (Coleoptera: Scarabaeidae). In these insects, however, epoxides are not involved in the biosynthetic pathway. Instead, the hydroxyl group for the lactonization step is introduced by an enantioselective 8-hydroxylation of the fatty acid chain (47).

Our results point to the rectal papillae as the exact the site of HDL biosynthesis that hitherto had been assumed to serve primarily for water and electrolyte resorption (40). Because males of many parasitic wasps do hardly feed as adults, this part of the gut might have evolved to function in sexual communication. Our histological data suggest that the pheromone is secreted from the epithelial papillae to the lumen of the rectal vesicle and is released via the anal orifice. We regularly observed males tapping their abdomen on the ground leaving smeary traces that were attractive for virgin females (J.R., unpublished data). In some fruit flies (Diptera: Tephritidae), males convert in the rectal gland externally acquired methyleugenol to sex pheromone components (48), and some ants (Hymenoptera: Formicidae) produce trail pheromones in the rectal gland (49). In males of some parasitic wasps of the taxon Braconidae, the rectum is fused with the seventh metasomal tergum to a sponge-like structure that presumably serves volatile release (41). The present study, however, is proof of the rectal vesicle as a sex pheromone producing gland in Hymenoptera. We expect this finding to open the door for a better understanding of the reproductive biology of parasitic Hymenoptera. Comparative studies are needed to determine whether the biosynthesis of sex pheromones in the male intestinal tract is a common feature in this important group of insects.

Materials and Methods

Insects. *N. vitripennis* wasps were reared on puparia of *Lucilia caesar* as described in ref. 37.

Localization of the Pheromone Gland. Abdominal tips of single 3-day old males were excised together with the adjacent interior tissue and transferred to a drop of water (Fig. 1*A*). Interior genitalia (testis, seminal vesicle, and accessory gland) and rectal vesicle were detached from each other and extracted separately for 30 min with 20 μl of dichloromethane containing 20 ng/μl methyl undecanoate (Sigma–Aldrich) as an internal standard ($n = 10$). Aliquots of 1 μl were used for GC-MS analysis.

Synthesis of (±)-[$^{13}C_{18}$]-Erythro-Vernolic Acid. The labeled pheromone precursor (±)-[$^{13}C_{18}$]-erythro-vernolic acid was synthesized from [$^{13}C_{18}$]-linoleic acid by epoxidation in dichloromethane with *m*-chloroperbenzoic acid (for more details see *SI Text*). The mass spectrum of the methylated synthesis product is shown in Fig. S4.

^{13}C-Labeling Experiments. Single 2-day-old parasitoid males were immobilized on an ice bath, and 0.1 μl of a solution containing 10 μg/μl (±)-[$^{13}C_{18}$]-*erythro*-vernolic acid dissolved in acetone was applied to the abdominal tip ($n = 5$), using a 5-μl microsyringe designed for GC on-column injection (Hamilton). The pure solvent ($n = 5$) was applied to control wasps. The next morning males were killed by freezing (−80°C), and dissected abdomens were extracted for 30 min with 20 μl of dichloromethane. Aliquots of 1 μl were used for GC-MS analysis.

Chemical Analysis. Abdomen and gland extracts were analyzed by GC-MS, using the instrumentation and conditions described in ref. 37. Quantification of pheromone components in the extracts was done by relating their peak areas to the internal standard.

Cloning of the Putative *N. vitripennis* EH Gene. Genomic DNA was extracted from adult males and used as a template to amplify the different PCR products in this study. Forty 3-day-old males were frozen and smashed into fine powder under liquid nitrogen. The powder was resuspended, and genomic DNA was extracted as described in ref. 50. At first, genomic DNA (100 ng/μl) was used as a template in combination with the degenerated primers Nas.EH1.dF1-Nas.EH1.dR1 (Fig. S1), which were synthesized from *Apis mellifera* predicted EH gene sequences (GenBank accession no. XM_394922). Subsequently, the genomic DNA was composed as template with the Nas.EH1.F1, 2, 3, and 4 −Nas.EH1.R1, 2, 3, and 4 primers, respectively (Fig. S1), to amplify the complete CDS of the gene. The PCR program was as follows: 95°C for 5 min,

followed by 10 cycles of 94°C for 20 sec; 65°C for 45 sec, decreasing by 0.5°C per cycle and 68°C for 2 min, followed by 35 cycles of 94°C for 30 sec; 60°C for 45 sec; 68°C for 2 min; and a final extension step of 68°C for 10 min.

All of the amplified DNAs were eluted from agarose gel (Roth), using the Wizard SV Gel and PCR cleaning system (Promega), and ligated into plasmids with the pGEM -Teasy Vector System supplied with JM109 competent cells (Promega) for amplification. Plasmid DNAs were later purified by using Pureyield Plasmid Midiprep system kit, following manufacturer's instructions (Promega). The PCR products were sequenced by MWG Biotech.

Phylogenetic Analysis of Insect Epoxide Hydrolase Genes. Neighbor-joining tree analysis of the amino acid sequences predicted from insect EH genes was performed for the species indicated in Fig. S5. All sequences were downloaded from the genomic DNA archive database at the National Center for Biotechnology Information (www.ncbi.nih.gov/blast/agtrace.html). Alignment analyses were performed by means of the AlignX server (www.ebi.ac.uk/clustalw). The corrected distance of tree was rooted by declaring the *Drome-mEH* and its homolog (*Drome-JHEH2*) as outgroup based on its role as homolog to insect JHEH (26). The neighbor joining tree was produced and the tree was drawn as described in ref. 50.

Tissue-Specific Localization, Using Whole-Mount *in Situ* RT-PCR Analysis. Rectal vesicles were prepared from 2-day-old adult males and immediately fixed in fixation buffer [4% paraformaldehyde in 1× DEPC-PBS buffer (130 mM NaCl, 7 mM Na_2HPO_4, and 3 mM NaH_2PO_4)] overnight at 4°C. Fixed tissues were dehydrated in an ethanol series of 30, 50, 70, 95, and 96% (vol/vol) ethanol/water, followed by protein digestion, using proteinase K (2 μg/ml) for 7 min. After dehydration, the tissues were treated following the protocol of ref. 51 up to the *in situ* RT-PCR step. To each single tissue, 20 μl of a one-step RT-PCR solution composed of reverse transcriptase buffer, chelate buffer, $MnCl_2$, $MgCl_2$, dNTPs, dig 11-dUTP (Roche), primers Nas.EH1.F1 and Nas.EH1.R1 (10 pmol/μl) (Fig. S1), Tth DNA polymerase, and water was added. The *in situ* RT-PCR was performed with the temperature profile of 60 min at 50°C, 5 min of 95°C, 35 cycles of 30 sec at 94°C, 1 min at 60°C, and 1 min at 68°C. Further steps were performed as done in ref. 51.

Synthesis of *Nasvi-EH1 and Nasvi-EH2* Double-Stranded RNA. dsRNA of the *Nasvi-EH1* and *Nasvi-EH2* genes were synthesized as described in ref. 52 with some modifications. The plasmids Nas.EH1.F1-Nas.EH1.R1 and Nas.EH2.F1-Nas.EH2.R1 (Figs. S1 and S6*B*) were linearized with PstI and SacI (25 units/μl; Promega), respectively. Linearization sites were previously identified by using peptide cleavage site recognition analysis server (www.expasy.ch/cgi-bin/peptidecutter/peptidecutter.pl). The linearized plasmids were recovered as described in ref. 51 and 1 μg from each linearized DNA plasmid was transcribed *in vitro* into dsRNA, using MEGAscript High Yield Transcript Kit, according to the manufacturer protocol (Ambion). The dsRNAs were purified by using phenol:chloroform extraction and isopropanol precipitation and subsequently resuspended in 50 μl of DEPC water. Quality of dsRNAs was examined by running 1 μl of each precipitated RNA on a 1% agarose gel containing 0.5 μg/ml^{-1} ethidium bromide. Concentration of dsRNA probes was adjusted to 400 ng/μl, using 1× DEPC-PBS buffer and stored at −80°C until use.

One microgram of each linearized DNA plasmid was also transcribed *in vitro* into RNA, using the RNAMaxx High Yield transcription kit, following the manufacturer's recommendations (Stratagene). The RNAs were purified by using Stratagene's Absolutely RNA RT-PCR Miniprep kit, resuspended in 50–100 μl of DEPC water and stored at −80°C until used as internal standard for quantitative real time RT-PCR analysis.

RNAi Experiments. *N. vitripennis* males emerge with almost no HDL and pheromone biosynthesis increases within the first 2 days (37). Therefore, freshly emerged males of equal size were used for RNAi experiments. Microinjection of dsRNA corresponding to *Nasvi-EH1* (n = 18), *Nasvi-EH2* (control 1, n = 16), or 1× DEPC-PBS buffer (control 2, n = 18) into adult wasps was done by using a modified protocol developed for *N. vitripennis* pupae (52). For fixation, males were carefully pushed backward into micropipette tips (eptips, 0.5–20 μl, Eppendorf), using a fine needle and a small plug of cotton wool. The lower end of the tip had been cut off with a scalpel so that the abdomen poked out of the tip but the wasps were not able to escape. A micropipette tip containing a male wasp was fixed under a stereo microscope, using modeling clay. The microinjection needle was inserted into the abdominal tip of the male and dsRNA was injected by gently pressing the plunger until the abdomen visibly swelled. The needle was carefully withdrawn 20 sec later. The pheromone was extracted 48 h after injection as described above and quantified by GC-MS analysis.

Quantitative Real-Time RT-PCR Analysis. Rectal vesicle tissues from 48-h-old males treated with dsRNAs corresponding to the two putative EH genes (n = 6 for each gene) or for control with DEPC-PBS buffer (n = 6) (see above) were dissected under Ringer solution (pH 7.0), frozen directly by using liquid nitrogen, and stored at −80°C until used for RNA analysis. RNA samples from single tissues were isolated by using Micro RNA Isolation Kit, as recommended by the manufacturer (Stratagene) in combination with DNase treatment (RQ1 RNase-free DNase; Promega) to remove potential genomic DNA contaminations. The RNA samples were adjusted to a concentration of 10 ng/μl with DEPC water and stored at −80°C until use. Quantitative real time RT-PCRs of the *Nasvi-EH1* gene were performed in a reaction volume of 20 μl including 6.65 μl of DEPC water, 10 μl of 2x FullVelocity SYBR green Q-RT-PCR master mix, 0.3 μl of diluted reference dye, 0.05 μl of StrataScript RT/RNase block enzyme mixture (Stratagene), 1 μl of RNA, and 1 μl of each of primers Nas.EH1.F1 and Nas.EH1.R1 (20 pmol/μl). For *Nasvi-EH2* gene analysis, 1 μl of the primers Nas.EH2.F1 and Nas.EH2.R1 (20 pmol/μl) was used (Fig. S6). *In vitro* RNA of Nas.EH1.F1-Nas.EH1.R1 or Nas.EH2.F1-Nas.EH2.R1 was used to generate internal standard curves.

Histology. Abdomens of 2-day-old males were fixed in Karnovsky solution [2.5% glutaraldehyde and 3.2% formaldehyde in 0.1M phosphate buffer with 0.1 M NaCl (pH 7.2)] overnight at 4°C. After postfixation in a buffered osmium tetroxide-solution (1%) for 45 min at 4°C, fixed materials were dehydrated in a graded acetone-series and embedded via the intermedium propylene oxide into Araldite epoxy resin (Fluka). Hardening of the resin at 60°C was accelerated by adding benzyldimethylamine (BDMA) (composition Araldite:hardener:BDMA 1:1:0.06). Series of semi thin sections (0.7 μm) were made on a Reichert Ultracut E microtome (Leica). The sections were stained with 1% toluidine, embedded into DepeX, and examined with an Olympus BX 50 light microscope equipped with a Colorview II digital camera.

ACKNOWLEDGMENTS. We thank Monika Hilker for making laboratory facilities available and two anonymous reviewers for helpful comments. This research was funded by the Deutsche Forschungsgemeinschaft Grant RU-717/8-1 and Heisenberg Fellowship of the Deutsche Forschungsgemeinschaft Grant RU-717/7-1 (to J.R.).

1. Hardie J, Minks AK (1999) *Pheromones of Non-Lepidopteran Insects Associated with Agricultural Plants* (CABI, Wallingford, CT).
2. Wyatt TD (2003). *Pheromones and Animal Behaviour* (Cambridge Univ Press, Cambridge).
3. Ma PWK, Ramaswamy SB (2003) Biology and ultrastructure of sex pheromone-producing tissue. *Insect Pheromone Biochemistry and Molecular Biology*, eds Blomquist G, Vogt R (Elsevier, London), pp 19–51.
4. Tillman JA, Seybold SJ, Jurenka RA, Blomquist GJ (1999) Insect pheromones—an overview of biosynthesis and endocrine regulation. *Insect Biochem Mol Biol* 29:481–514.
5. Jurenka RA (2004) Insect pheromone biosynthesis. *Top Curr Chem* 239:97–132.
6. Bjostad LB, Roelofs WL (1983) Sex pheromone biosynthesis in *Trichoplusia ni*: Key steps involve delta-11 desaturation and chain-shortening. *Science* 220:1387–1389.
7. Morse DAVI, Meighen EDWA (1984) Aldehyde pheromones in Lepidoptera: Evidence for an acetate ester precursor in Choristoneura fumiferana. *Science* 226:1434–1436.
8. Adams TS, Dillwith JW, Blomquist GJ (1984) The role of 20-hydroxyecdysone in housefly sex-pheromone biosynthesis. *J Insect Physiol* 30:287–294.
9. Cusson MICH, McNeil JN (1989) Involvement of juvenile hormone in the regulation of pheromone release activities in a moth. *Science* 243:210–212.
10. Raina AK, *et al.* (1989) Identification of a neuropeptide hormone that regulates sex pheromone production in female moths. *Science* 244:796–798.
11. Chase J, Touhara K, Prestwich GD, Schal C, Blomquist GJ (1992) Biosynthesis and endocrine control of the production of the German cockroach sex pheromone 3,11-dimethylnonacosane-2-one. *Proc Natl Acad Sci USA* 89:6050–6054.
12. Rafaeli A, Jurenka RA (2003) PBAN regulation of pheromone biosynthesis in female moths. *Insect Pheromone Biochemistry and Molecular Biology*, eds Blomquist G, Vogt R (Elsevier, London), pp 107–136.
13. Jurenka RA (2003) Biochemistry of female moth sex pheromones. *Insect Pheromone Biochemistry and Molecular Biology*, eds Blomquist G, Vogt R (Elsevier, London), pp 53–80.
14. Jallon J-M, Wicker-Thomas C (2003) Genetic studies on pheromone production in Drosophila. *Insect Pheromone Biochemistry and Molecular Biology*, eds Blomquist G, Vogt R (Elsevier, London), pp 253–282.
15. Roelofs WL, Rooney AP (2003) Molecular genetics and evolution of pheromone biosynthesis in Lepidoptera. *Proc Natl Acad Sci USA* 100:9179–9184.
16. Tittiger C (2003) Molecular biology of bark beetle pheromone production and endocrine regulation. *Insect Pheromone Biochemistry and Molecular Biology*, eds Blomquist G, Vogt R (Elsevier, London), pp. 201–230.

17. Moto K, *et al.* (2003) Pheromone gland-specific fatty-acyl reductase of the silkmoth, Bombyx mori. *Proc Natl Acad Sci USA* 100:9156–9161.
18. Moto K, *et al.* (2004) Involvement of a bifunctional fatty-acyl desaturase in the biosynthesis of the silkmoth, Bombyx mori, sex pheromone. *Proc Natl Acad Sci USA* 101:8631–8636.
19. Gilg AB, Bearfield JC, Tittiger C, Welch WH, Blomquist GJ (2005) Isolation and functional expression of an animal geranyl diphosphate synthase and its role in bark beetle pheromone biosynthesis. *Proc Natl Acad Sci USA* 102:9760–9765.
20. Matsumoto S, Hull JJ, Ohnishi A, Moto K, Fonagy A (2007) Molecular mechanisms underlying sex pheromone production in the silkmoth, Bombyx mori: Characterization of the molecular components involved in bombykol biosynthesis. *J Insect Physiol* 53:752–759.
21. Hall GM, *et al.* (2002) Midgut tissue of male pine engraver, Ips pini, synthesizes monoterpenoid pheromone component ipsdienol de novo. *Naturwissenschaften* 89:79–83.
22. Chertemps T, Duportets L, Labeur C, Ueyama M, Wicker-Thomas C (2006) A female-specific desaturase gene responsible for diene hydrocarbon biosynthesis and courtship behaviour in Drosophila melanogaster. *Insect Mol Biol* 15:465–473.
23. Ohnishi A, Hull JJ, Matsumoto S (2006) Targeted disruption of genes in the Bombyx mori sex pheromone biosynthetic pathway. *Proc Natl Acad Sci USA* 103:4398–4403.
24. Roelofs WL (1995) Chemistry of sex attraction. *Proc Natl Acad Sci USA* 92:44–49.
25. Morisseau C, Hammock BD (2005) Epoxide hydrolases: Mechanisms, inhibitor designs, and biological roles. *Annu Rev Pharmacol Toxicol* 45:311–333.
26. Newman JW, Morisseau C, Hammock BD (2005) Epoxide hydrolases: Their roles and interactions with lipid metabolism. *Progr Lipid Res* 44:1–51.
27. Khlebodarova TM, *et al.* (1996) A comparative analysis of juvenile hormone metabolizing enzymes in two species of Drosophila during development. *Insect Biochem Mol Biol* 26:829–835.
28. Wojtasek H, Prestwich G (1996) An insect juvenile hormone-specific epoxide hydrolase is related to vertebrate microsomal epoxide hydrolases. *Biochem Biophys Res Commun* 220:323–329.
29. Prestwich GD, Graham SM, König WA (1989) Enatioselective opening of (+)-disparlure and (−)-disparlure by epoxide hydrase in gypsy-moth antennae. *J Chem Soc Chem Commun* 9:575–577.
30. Plettner E, Slessor KN, Winston ML, Oliver JE (1996) Caste-selective pheromone biosynthesis in honeybees. *Science* 271:1851–1853.
31. Plettner E, Slessor KN, Winston ML (1998) Biosynthesis of mandibular acids in honey bees (Apis mellifera): De novo synthesis, route of fatty acid hydroxylation and caste selective beta-oxidation. *Insect Biochem Mol Biol* 28:31–42.
32. Blomquist G, Howard RW (2003) Pheromone biosynthesis in social insects. *Insect Pheromone Biochemistry and Molecular Biology*, eds Blomquist G, Vogt R (Elsevier, London), pp 323–340.
33. Luxova A, Valterova I, Stransky K, Hovorka O, Svatos A (2003) Biosynthetic studies on marking pheromones of bumblebee males. *Chemoecology* 13:81–87.
34. Quicke DLJ (1997) *Parasitic Wasps.* (Chapman and Hall, London).
35. Beukeboom L, Desplan C (2003) Nasonia. *Curr Biol* 13:R860.
36. Whiting AR (1967) Biology of the parasitic wasp Mormoniella vitripennis [=Nasonia brevicornis] (WALKER). *Quart Rev Biol* 42:333–406.
37. Ruther J, Stahl LM, Steiner S, Garbe LA, Tolasch T (2007) A male sex pheromone in a parasitic wasp and control of the behavioral response by the female's mating status. *J Exp Biol* 210:2163–2169.
38. Ruther J, Steiner S, Garbe LA (2008) 4-Methylquinazoline is minor component of the male sex pheromone in Nasonia vitripennis. *J Chem Ecol* 34:1–4.
39. Albrecht W, Tressl R (1993) Microbial transformation of (−)-vernolic acid into (4*R*,5*R*)-5-hydroxy-gamma-decalactone. *Tetrahedron Asymmetry* 4:1391–1396.
40. Davies I, King PE (1975) Structure of rectal papilla in a parasitoid hymenopteran Nasonia vitripennis (Walker) (Hymenoptera Pteromalidae). *Cell Tiss Res* 161:413–419.
41. Quicke DLJ, Wharton RA, Sitteritz-Bhatkar H (1996) Recto-tergal fusion in the Braconinae (Hymenoptera: Braconidae): Structure and distribution. *J Hym Res* 5:73–79.
42. Blee E, Schuber F (1990) Efficient epoxidation of unsaturated fatty acids by a hydroperoxide-dependent oxygenase. *J Biol Chem* 265:12887–12894.
43. Blee E, Schuber F (1995) Stereocontrolled hydrolysis of the linoleic acis monoepoxide regioisomers catalyzed by soybean epoxide hydrolase. *Eur J Biochem* 230:229–234.
44. Garbe LA, Tressl R (2003) Metabolism of deuterated isomeric 6,7-dihydroxydodecanoic acids in Saccharomyces cerevisiae—diastereo- and enantioselective formation and characterization of 5-hydroxydecano-4-lactone (=4,5-dihydro-5-(1-hydroxyhexyl)furan-2(3*H*)-one) isomers. *Helv Chim Acta* 86:2349–2363.
45. Gill SS, Hammock BD (1979) Hydration of cis- and trans-epoxymethyl stearates by the cytosolic epoxide hydrase of mouse liver. *Biochem Biophys Res Commun* 89:965–971.
46. Roy U, Loreau O, Balazy M (2004) Cytochrome P450/NADPH-dependent formation of trans epoxides from trans-arachidonic acids. *Bioorgan Med Chem* 14:1019–1022.
47. Leal WS, Zarbin PHG, Wojtasek H, Ferreira JT (1999) Biosynthesis of scarab beetle pheromones–enantioselective 8-hydroxylation of fatty acids. *Eur J Biochem* 259:175–180.
48. Khoo CCH, Tan KH (2005) Rectal gland of Bactrocera papayae: Ultrastructure, anatomy, and sequestration of autofluorescent compounds upon methyl eugenol consumption by the male fruit fly. *Microsc Res Tech* 67:219–226.
49. Hölldobler B, Wilson EO (1990) *The Ants.* (Harvard Univ Press, Cambridge, MA).
50. Abdel-Latief M (2007) A family of chemoreceptors in Tribolium castaneum (Tenebrionidae: Coleoptera). *PloS One* 12:e1319.
51. Abdel-Latief M, Hoffmann KH (2007) The adipokinetic hormones in the fall armyworm, Spodoptera frugiperda: cDNA cloning, quantitative real time RT-PCR analysis, and gene specific localization. *Insect Biochem Mol Biol* 37:999–1014.
52. Lynch JA, Desplan C (2006) A method for parental RNA interference in the wasp Nasonia vitripennis. *Nat Protocols* 1:486–494.